ACS OMEGA

http://pubs.acs.org/journal/acsodf

Article

Enhancement of the Mechanical Properties of Poly(lactic acid)/Epoxidized Soybean Oil Blends by the Addition of 3-Aminophenylboronic Acid

Jinyu Xie, Kai Gu, Yan Zhao, Jinrong Yao,* Xin Chen, and Zhengzhong Shao

Cite This: *ACS Omega* 2022, 7, 17841−17848

Read Online

ACCESS | Metrics & More | Article Recommendations | Supporting Information

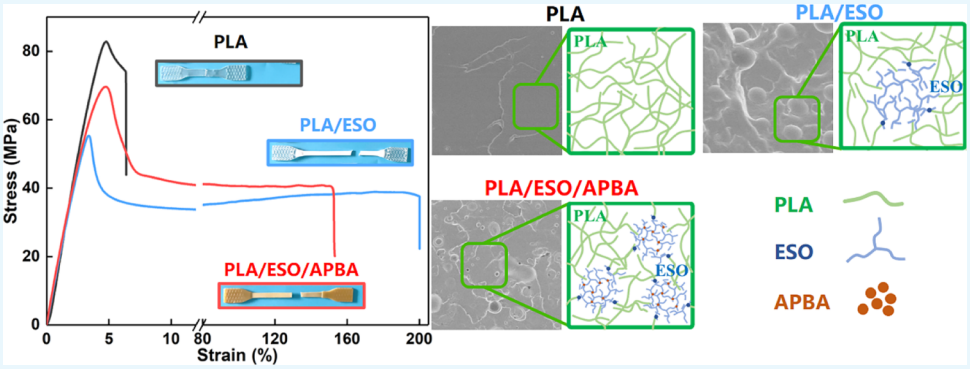

ABSTRACT: Here, the high-strength, high-ductility blends of poly(lactic acid) (PLA) with epoxidized soybean oil (ESO) and 3-aminophenylboronic acid (APBA) were successfully prepared via a melt-bending method. The effects of APBA addition on the mechanical and thermal properties, morphologies, and crystallization behavior of the blends were investigated. The results showed that the addition of APBA endowed the PLA/ESO/APBA blends with a good balance of strength and toughness. The yield strength of the PLA/ESO/APBA (90:10:3) blend was 70 MPa, which was 25% higher than that of the corresponding PLA/ESO blend without APBA (56 MPa), while its elongation at break reached 160%, which is greatly superior to that of pure PLA (6.5%). Scanning electron microscopy images showed that the incorporation of APBA significantly improved the compatibility between PLA and ESO, while gel permeation chromatography and rheological analysis suggested the occurrence of complex reactions between the three constituents, which improved the compatibility between PLA and ESO and enhanced the mechanical properties of the blends. Hence, the PLA/ESO/APBA blends possess great potential for application in the manufacture of environmentally friendly degradable plastics.

1. INTRODUCTION

The rapid development and wide application of polymer materials over the last several decades has led to excessive dependence on nonrenewable fossil resources[1,2] during manufacture, and the improper disposal of such materials has caused serious environmental pollution.[3,4] It is widely believed that these problems may be largely overcome by substituting traditional petroleum-based plastics with biopolymers derived from nature and degradable synthetic polymers.[5,6] Currently, poly(lactic acid) (PLA), a popular biodegradable polymer with good biocompatibility and high mechanical strength, has been widely studied and applied for this purpose.[7−9] However, the inherent brittleness and poor ductility of pure PLA limit its wide use, especially in applications where high toughness is required.[8,10]

To overcome the limitations of PLA-based materials, a number of methods such as chemical copolymerization and blending are currently being researched.[11,12] Blending, as the simplest method, is widely applied in the modification of PLA with plasticizers,[13] flexile polymers,[14,15] and copolymers.[16] Increasingly, to ensure the biodegradability of PLA-based blended materials, the use of degradable polymers and plasticizers from nature is preferred. Epoxidized plant oils (e.g., soybean oil and sunflower oil), as a type of green and nontoxic plasticizer, are often used in the plasticizing of polymer materials.[17,18] The epoxy group in the epoxidized plant oil can react with the terminal carboxyl or hydroxyl groups of PLA,[14] which helps to increase the interfacial interactions between the PLA and plasticizer. In comparison with PLA/soybean oil

Received: February 24, 2022
Accepted: May 9, 2022
Published: May 18, 2022

blends, the PLA/epoxidized soybean oil (ESO) blends show a significant increase in ductility.[17,19] Unfortunately, there is a large difference in strength between PLA/ESO blends and pure PLA. Hence, it is crucial to achieve a good balance between strength and toughness in blended PLA/ESO systems.

One approach to increasing the strength of polymer materials is through the addition of boric acid or boroxine compounds, which is often applied to polyolefins,[20,21] ethylene-vinyl acetate copolymer (EVA),[22] poly(aryl ether ketone),[23] and other polymer materials.[24,25] Owing to the ease of formation and reversible nature of borate ester bonds and the boroxine structure, dynamic cross-linking occurs between polymer chains, which contributes to the high mechanical strength of polymer materials.

Against this backdrop, the present study proposes the use of 3-aminophenylboronic acid (APBA) as an additive in the preparation of PLA/ESO materials with a balance between strength and toughness. The mechanical properties, morphologies, and thermal properties of the resulting PLA/ESO/APBA blends, and the crystallization behavior of PLA within the blends, were investigated using universal mechanical testing machines, field emission scanning electron microscopy (FESEM), differential scanning calorimetry (DSC), wide-angle X-ray diffraction (WAXD), and small-angle X-ray scattering (SAXS).

2. MATERIALS AND METHODS

2.1. Materials. PLA (4032D, 2% D-lactide) was supplied by NatureWorks LLC (USA). ESO, APBA, and 3-aminophenylboronic acid pinacol ester (APPE) were obtained from Aladdin Industrial Corporation (China). All the other chemicals used in this study were purchased from Sinopharm Chemical Reagent Co., Ltd. (China) and were used as received without further purification.

2.2. Preparation of PLA/ESO/APBA Blends. Prior to the blending modification, PLA, APBA, and APPE were dried at 50 °C for 18 h in a vacuum oven. To prepare the blends, PLA was first melted in a mixer (HAAKE Polylab OS, Thermo Fisher, USA) at a rotating speed of 60 rpm at 180 °C before adding ESO and APBA into the mixer at 1 and 4 min, respectively. After mixing for 8 min, the blend was cooled to a solid and cut into small pieces. Each sample was then compression molded into sheets with thicknesses of 1.0 or 3.0 mm using a press vulcanizer (GT 7014 H30C, Taiwan High Speed Rail Testing Instrument Co., Ltd., Taiwan, China) at 190 °C. Neat PLA, along with PLA/ESO and PLA/ESO/APPE blends, were prepared as control samples using the same method.

2.3. Characterization. *2.3.1. Mechanical Testing.* The tensile properties of neat PLA and its blends were tested using a universal testing machine (model 5966, Instron, USA) at a stretching speed of 10 mm/min, according to the ATSM D638 standard. A sensor with a range of 1 kN was selected, and the test temperature was 23 °C. The tensile specimens were dumbbell shaped, with a size of 20 mm × 4 mm × 1 mm. The results reported for each material composition were averaged from at least five specimens.

The Izod unnotched impact strength of PLA and its blends was tested using an impact testing machine (SS-3700CZ, Sungshu Testing Instrument Co., Ltd., Taiwan, China) according to the GB/T 1843-2008 standard at 23 °C. The size of the Izod unnotched impact test specimens was 80 mm × 10 mm × 3 mm. The results reported for each material composition were averaged from at least five specimens.

2.3.2. Field Emission Scanning Electron Microscopy. The micrographs of the cryo-fractured (in liquid nitrogen) surfaces of PLA and blends were acquired using FESEM (Zeiss Ultra-55, Germany) at an accelerating voltage of 1 kV. The fractured surfaces were sprayed with gold (10 mA, 60 s) prior to measurement.

2.3.3. Rheological Analysis. The rheological properties of PLA and its blends were measured using a rotational rheometer (HAAKE MARS III, Thermo Fisher, USA) on wafer-shaped samples with a diameter of 20 mm and a thickness of ∼1 mm. All the measurements were conducted at 190 °C under a nitrogen atmosphere. First, a dynamic strain scan was carried out to determine the linear viscoelastic region, followed by a dynamic frequency scan test in which the strain value was set at 1% and the scanning frequency range was 0.01−100 rad/s.

2.3.4. Gel Permeation Chromatography. The molecular weights of PLA and its blends were measured via gel permeation chromatography (GPC) (Agilent 1260, Germany), equipped with a Waters 2487 absorbance detector, a Waters 2414 refractive index detector, and three TSK gel columns with pore sizes of 15, 30, and 200 Å, respectively. Prior to the tests, the GPC instrument was calibrated using polystyrene standards and chloroform (1.0 mL/min) as the eluent.

2.3.5. Differential Scanning Calorimetry. The thermal properties of neat PLA and its blends were tested using DSC (Q2000, TA Instruments, USA) under a nitrogen atmosphere. The specimens were dried prior to testing, and the masses of the specimens were between 5 and 9 mg. The specimens were then heated from 0 to 190 °C at a rate of 10 °C/min and maintained at 190 °C for 3 min to eliminate the thermal history before being cooled to 0 °C at a rate of 10 °C/min and was held for another 3 min. After cooling, the specimens were reheated to 190 °C at a rate of 10 °C/min. The values of the glass transition temperature, T_g, cold crystallization temperature, T_{cc}, cold crystallization enthalpy, ΔH_{cc}, melting temperature, T_m, and melting enthalpy, ΔH_m, of the PLA were measured during the second heating curve. The crystallinity of the PLA, $X_{c,PLA}$, in the sample was evaluated as follows

$$X_{c,PLA}\ (\%) = \frac{\Delta H_m}{W_{PLA} \times \Delta H_m^0} \times 100\% \quad (1)$$

where ΔH_m is the observed melting enthalpy of PLA, W_{PLA} is the weight fraction of PLA in the blend, and ΔH_m^0 is the theoretical melting enthalpy of 100% crystalline PLA (=93 J/g).[26]

2.3.6. Thermogravimetric Analysis. The thermal stability of PLA and its blends was evaluated via thermogravimetric analysis (TGA) (Pyris 1, PerkinElmer, USA). Specimens weighing 3−5 mg were heated from 50 to 600 °C at a rate of 10 °C/min under a nitrogen atmosphere.

2.3.7. WAXD and SAXS. Prior to testing, the disk specimens of PLA and its blends (with a diameter of 20.0 mm and a thickness of 1.0 mm) were melted by heating at 190 °C for 10 min, then held at 130 °C for 6 h for isothermal crystallization, followed by cold pressing to cool to room temperature. WAXD measurements were performed using an X-ray diffractometer (D2 Phaser, Bruker, Germany) with a Cu Kα radiation source (40 kV, 200 mA). The scanning range of the diffraction angle (2θ) ranged from 10 to 30° with a scanning speed of 2°/min. The SAXS measurements were carried out using an SAXS system (Xeuss 2.0, Xenocs, France) with an Mo Kα radiation source at a diffraction angle (2θ) of 3.4° and a scattering vector ranging from 0.02 to 2.4 nm^{-1}. The samples were placed 2500 mm away

https://doi.org/10.1021/acsomega.2c01102
ACS Omega 2022, 7, 17841−17848

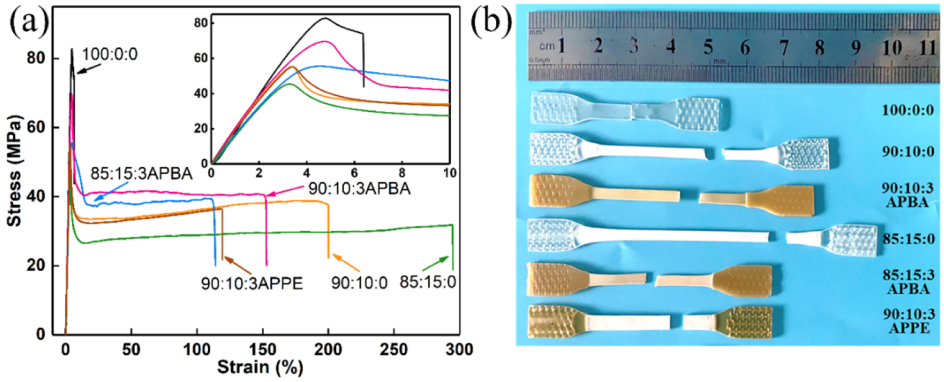

Figure 1. (a) Stress−strain curves of neat PLA and PLA-based blends. (b) Photographs of different samples after tensile tests.

Table 1. Mechanical Properties of Neat PLA and PLA-Based Blends

PLA/ESO/APBA (w/w/w)	yield strength (MPa)	tensile modulus (MPa)	tensile strength (MPa)	elongation at break (%)	impact strength (kJ/m^2)
100:0:0	83.2 ± 1.9	2200 ± 54	74.3 ± 3.0	6.5 ± 0.4	16.54 ± 0.84
90:10:0	56.0 ± 0.8	1920 ± 19	37.0 ± 2.3	200 ± 16	32.22 ± 2.89
85:15:0	45.9 ± 1.1	1720 ± 33	31.5 ± 2.4	290 ± 40	46.83 ± 2.16
90:10:3	70.3 ± 0.6	2100 ± 16	41.7 ± 0.8	160 ± 30	25.23 ± 2.24
85:15:3	55.2 ± 0.6	1710 ± 30	39.3 ± 0.2	114 ± 14	28.71 ± 1.66
90:10:3 (APPE)	54.9 ± 2.4	1940 ± 58	37.2 ± 1.5	124 ± 16	19.32 ± 1.73

from the detector, and the signal acquisition time for each sample was 30 min.

2.3.8. Dynamic Mechanical Analysis. The dynamic mechanical properties of PLA and its blends were measured using a dynamic mechanical analyzer (SDTA861e, Mettler Toledo, Switzerland) under a large tensile mode at a frequency of 1 Hz. The rectangular samples (10.5 mm × 4 mm × 1 mm) were heated from 0 to 120 °C at a heating rate of 3 °C/min.

2.3.9. Dissolve-precipitation Test of Blends. 2.0 g of PLA/ESO (85:15) and PLA/ESO/APBA (85:15:3) blends were dissolved in 15 mL of chloroform, respectively. Then, the chloroform solution was poured into 200 mL of anhydrous ethanol and kept at −30 °C for 24 h. After filtration or centrifugation, the precipitate is separated. Finally, the soluble part of the blend in the filtration liquid was recovered by rotary evaporation. The abovementioned residue recovered from the filtration liquid was re-dissolved in chloroform and coated onto a potassium bromide disk for Fourier transform infrared (FT-IR) analysis.

2.3.10. FT-IR Spectroscopy and Nuclear Magnetic Resonance Spectroscopy. The FT-IR spectra were recorded on a FT-IR spectrometer (Nicolet 6700, Thermo Fisher, USA) with a wavenumber of 4000-500 cm^{-1}, at a resolution of 4 cm^{-1} and 64 scans.

A ^{1}H nuclear magnetic resonance (NMR) spectrum of the residue recovered from the filtration liquid was obtained on a 400 MHz spectrometer (AVANCE III HD, Bruker, Switzerland), using $CDCl_3$ as the solvent and tetramethylsilane as the internal standard.

3. RESULTS AND DISCUSSION

3.1. Preparation of PLA/ESO/APBA Blends. PLA/ESO blends and PLA/ESO/APBA blends were prepared via melt blending in a HAAKE mixer at a speed of 60 rpm at 190 °C. The change in melt torque during blending can be used to gain a preliminary understanding of the character of the reaction between PLA, ESO, and APBA (Figure S1 of the Supporting Information).[14,27] In comparison with the torque curve of pure PLA, the torque significantly decreased within 2 min of ESO addition, which is similar to the behavior observed when adding common plasticizers.[28,29] As the mixing time increased, the torque increased and tended toward a stable value due to the reaction between the carboxyl or hydroxyl groups of PLA and the epoxy groups of ESO. The torque further increased following the addition of APBA at 4 min, before tending toward a stable value. The significant increase in torque in the presence of APBA is attributed to the complex reactions between PLA, ESO, and APBA (which will be discussed in more detail in Section 3.5). Moreover, the increase in the torque of PLA/ESO blends with APBA translates to an enhancement in the melt strength, which is beneficial for material processing.

The addition of APBA has great influence on the mechanical properties of the PLA/ESO blends (Figure S2). The yield strength of PLA/ESO/APBA samples was higher than that of PLA/ESO blends with the same ESO content and increased with the increase of APBA, while the elongation was inferior to that of samples without APBA. It is obvious that the samples with an APBA content of 3 phr (parts per hundred of the PLA and ESO mixture) had a relatively balanced yield strength and elongation at break. Hence, these samples with 3 phr of APBA were selected for subsequent performance characterization.

3.2. Mechanical Properties of PLA/ESO/APBA Blends. Figure 1 shows the typical stress−strain curves of the PLA-based blends, and the data are summarized in Table 1. The results show that neat PLA has excellent yield strength (83.2 MPa) and tensile modulus (2200 MPa), which is comparable to the mechanical properties of general plastics. However, its elongation at break is very low (6.5%), and its impact strength is only 16.54 kJ/m^2. With the addition of ESO, the elongation at break and impact strength were significantly improved (by over 200%), whereas the tensile modulus and yield strength decreased significantly in comparison with PLA, which is consistent with the literature.[18,30,31]

The addition of APBA further improved the mechanical properties of the resulting PLA/ESO/APBA blends, with an

https://doi.org/10.1021/acsomega.2c01102
ACS Omega 2022, 7, 17841−17848

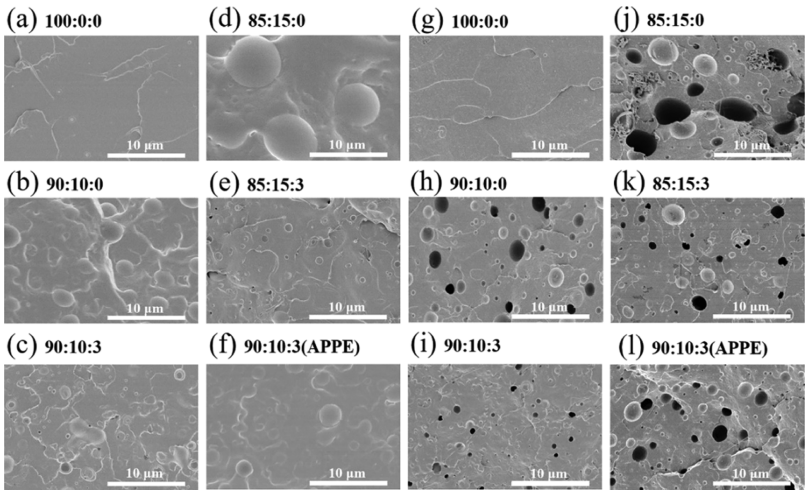

Figure 2. SEM micrographs of cryo-fractured surfaces of neat PLA and PLA-based blends: (a–f) untreated samples, (g–l) after soaking in ethanol for 24 h.

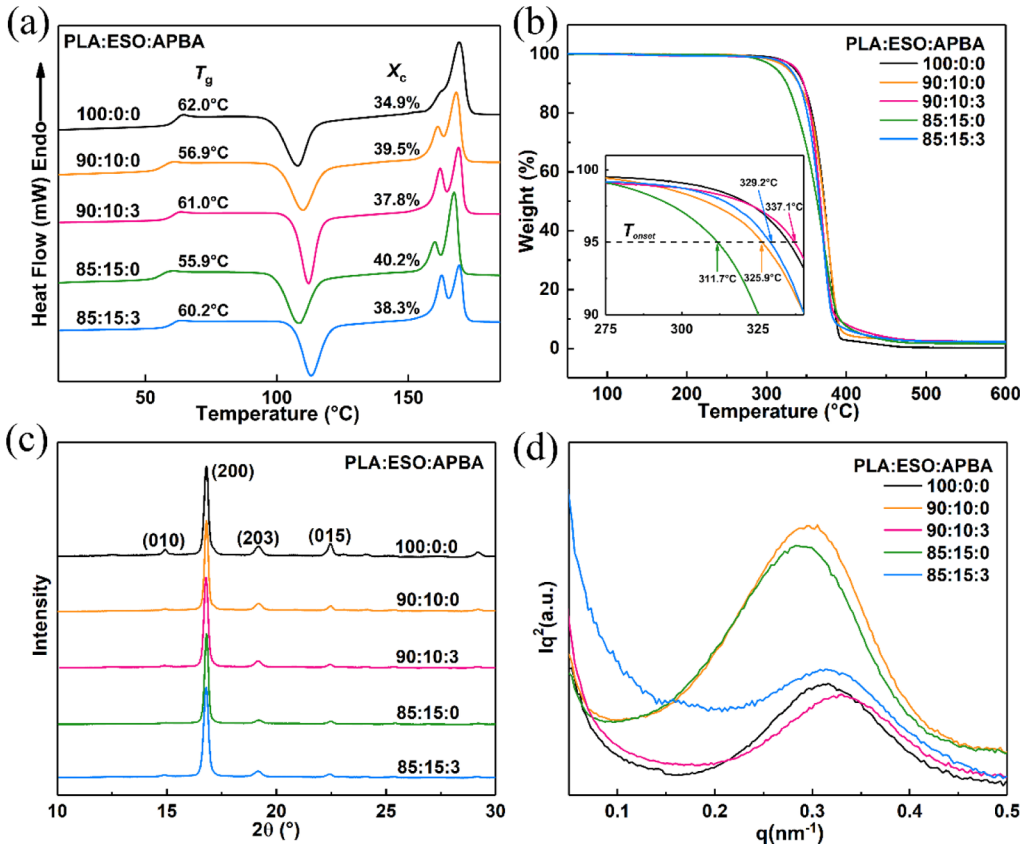

Figure 3. (a) DSC curves of neat PLA and PLA-based blends for the second heating run. (b) TGA curves, (c) WAXD patterns, and (d) SAXS patterns of different blends.

increase in the yield strength of over 20% compared to PLA/ESO. For instance, the yield strength of the PLA/ESO/APBA blend (90:10:3) was 70 MPa, which is significantly higher than that of the corresponding blend without APBA (56 MPa). Furthermore, the breaking strain and Izod impact strength were 160% and 25.23 kJ/m^2, respectively. The yield strength and elongation at break of PLA/ESO/APBA blends are close to those of PLA/rubber blends.[11,32,33] Generally, the presence of amino group-containing compounds will cause serious degradation of PLA during the melting process, resulting in a marked deterioration in mechanical properties. Therefore, the boric acid groups of APBA are expected to play an important role in increasing the yield strength of the PLA/ESO/APBA blends. Unfortunately, the blends with ABPA became nontransparent with a khaki color, which may limit the application of blends in transparent packaging and those fields with high requirements for material color.

To verify the effect of the boric acid groups in APBA on the enhancement of mechanical properties, APPE was added into the PLA/ESO system as a substitute for APBA. As Table 1

https://doi.org/10.1021/acsomega.2c01102
ACS Omega 2022, 7, 17841−17848

Table 2. Thermal Properties and Crystal Layer Thicknesses, d_c, of Neat PLA and PLA-Based Blends

PLA/ESO/APBA (w/w/w)	T_g (°C)[a]	T_{cc} (°C)[a]	ΔH_{cc} (J/g)	T_m (°C)[a]	ΔH_m (J/g)	X_c (%)[a]	q_{max} (nm^{-1})[b]	d_c (nm)[b]
100:0:0	62.0	107.7	26.32	169.3	29.36	34.9	0.315	11.7
90:10:0	56.9	109.8	30.04	168.3	33.08	39.5	0.297	13.4
90:10:3	61.0	112.2	31.38	169.1	30.76	37.8	0.331	11.7
85:15:0	55.9	108.4	30.41	167.4	31.79	40.2	0.291	14.4
85:15:3	60.2	113.1	29.11	169.3	29.38	38.3	0.325	12.2

[a]Obtained from the DSC curves for the second heating run. [b]Obtained from the SAXS curves.

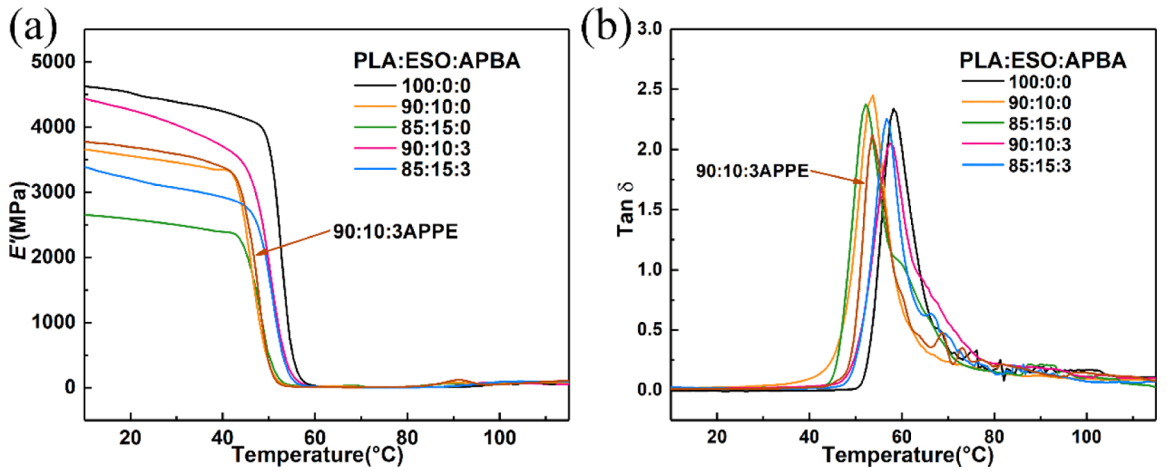

Figure 4. Dynamic mechanical properties of neat PLA and PLA-based blends: (a) storage modulus, E', and (b) tan δ.

shows, the yield strength and tensile modulus of the PLA/ESO/APPE blend (90/10/3) was not significantly different to that of the PLA/ESO blend (90/10), whereas the elongation at break decreased from ~200 to 124%. This finding confirms that the boric acid groups in APBA contribute to the enhancement of the mechanical properties of PLA/ESO blends.

3.3. Morphology of PLA/ESO/APBA Blends. The morphologies of the cryo-fractured surfaces of neat PLA and the PLA/ESO, PLA/ESO/APBA, and PLA/ESO/APPE blends observed using FESEM are shown in Figure 2, whence it can be seen that the fractured surface of neat PLA was smooth and uniform (Figure 2a). After blending with ESO, however, spherical particles were observed on the fractured surfaces of the PLA/ESO blends, and the particle sizes were positively correlated with ESO concentration (Figure 2b,d). When APBA was introduced into the PLA/ESO blends, the size of the spherical particles decreased significantly, and the interface between the particle and the matrix became somewhat ambiguous (Figure 2c,e).

To remove any ESO and APBA molecules in the blended samples that were unbonded on PLA, the fractured blend sheets were immersed in ethanol for 24 h. The SEM images of the resulting fracture surfaces of the blends (Figure 2g–l) show that many holes appeared in the PLA/ESO blends following ethanol treatment. For the PLA/ESO/APBA blends, however, the diameter and number of holes on the fractured surfaces were noticeably reduced. These results confirm that the addition of APBA significantly improved the compatibility between PLA and ESO, which likely explains the improved mechanical properties of PLA/ESO/APBA blends.

3.4. Thermal and Crystallization Properties of PLA/ESO/APBA Blends. The thermal properties of neat PLA and PLA/ESO and PLA/ESO/APBA blends were investigated using DSC (Figure 3a and Table 2). The results show that the glass transition temperature, T_g, of PLA in the PLA/ESO blends decreased from ~62 °C for pure PLA to 56 °C at 15% ESO content, while the crystallinity of PLA, $X_{c,PLA}$, gradually increased due to the improved mobility of PLA chains caused by the plasticization of ESO. After APBA was introduced, the T_g of PLA in the PLA/ESO/APBA blends became closer to that of pure PLA, while its crystallinity slightly decreased. Dynamic mechanical analysis (DMA) of the blends further confirmed these significant changes in T_g (Figure 4). The DMA results show that both the storage modulus, E', and T_g of the blends decreased significantly with the increasing ESO content but increased with the addition of APBA. When APBA was replaced by APPE, E' and T_g of the blend were not significantly different to those of the PLA/ESO blend with the same ESO content. Additionally, double melting peaks were observed in all the DSC curves of the PLA blends. For the PLA/ESO/APBA blends, the intensity of the lower-temperature melting peak, which is attributed to the imperfect crystalline form of PLA,[34−36] was higher than that of PLA/ESO blends with the same ESO content. These results indicate that the incorporation of APBA into the PLA/ESO blends hindered the movement of PLA chains, resulting in an increase in T_g and the formation of greater amounts of imperfect crystalline PLA. In addition, from the TGA curves (Figures 3 and 4b), the onset degradation temperature (T_{onset}) of PLA/ESO/APBA blends was higher than that of PLA/ESO blends with the same ESO content. It means that the thermal stability of PLA/ESO blends has been enhanced with the addition of APBA.

The WAXD patterns of PLA (Figure 3c) showed four main diffraction peaks at ~14.9, 16.8, 19.1, and 22.4°, corresponding to the (010), (200), (203), and (015) lattice planes of PLA, respectively, which are assigned to the typical α phase of crystalline PLA.[37] In addition, similar diffraction peaks were observed in the WAXD patterns of the PLA/ESO and PLA/

https://doi.org/10.1021/acsomega.2c01102
ACS Omega 2022, 7, 17841−17848

ESO/APBA blends, indicating that the crystal morphology of PLA in the blends was unchanged. The crystalline structure of the PLA component in the PLA/ESO/APBA blends was further investigated via SAXS (Figure 3d), and the data are summarized in Tables 2 and S1. The results show that the PLA component in all the blends possessed a broad scattering peak at around q = 0.31 nm^{-1}. From the results calculated using Bragg's equation, the crystal layer thickness, d_c, of PLA was positively correlated with the ESO content but negatively correlated with that of APBA. The reduction in d_c further confirms that the introduction of APBA reduced the crystalline ability of PLA chains in the blends.[14] These changes in the thermal properties and crystallization behavior of PLA may be attributed to the complex reactions between PLA, ESO, and APBA, which affect both the compatibility between PLA and ESO and the movements of the molecular chains.

3.5. Supposed Mechanism of Compatibility Enhancement. PLA will degrade under melt-blending conditions (190 °C), leading to a decrease in its molecular weight, M_n, from 176,000 to 152,000 g/mol (Table 3). After adding ESO, epoxy groups reacted with the terminal carboxyl or hydroxyl groups of PLA (Figure 5).[27] This results in plasticization causing the storage modulus, G', loss modulus, G'', and complex viscosity, η^*, of the PLA/ESO blends to significantly decrease (Figure S3).

Table 3. Molecular Weights and Polydispersity Indexes of Neat PLA and PLA-Based Blends

samples	M_n (g/mol)[a]	PDI[a]
pristine PLA (pellets)	176,000	1.71
neat PLA (100:0:0)	152,000	1.80
PLA/ESO (90:10:0)	149,000	1.89
PLA/ESO/APBA (90:10:3)	133,000	1.85
PLA/ESO/APPE (90:10:3)	116,000	1.73

[a]Obtained from GPC with chloroform as the eluent.

During the preparation of PLA/ESO/APBA blends, APBA (which was added 3 min after ESO) was able to connect with ESO via the reaction between its amino groups and the epoxy groups of ESO (Figure 5). Simultaneously, APBA can link up with the PLA chains via the aminolysis of esters, resulting in serious degradation of PLA and a decrease in M_n to 133,000 g/mol. When APPE was used in place of APBA, the M_n of PLA decreased to 116,000 g/mol, which meant more serious degradation of PLA had happened. Moreover, when the chloroform solution of the PLA/ESO (85:15) or PLA/ESO/APBA (85:15:3) blend was precipitated by ethanol, some residue could be recovered from the filtration liquid. As confirmed by FT-IR (Figure S4) and ^1H NMR spectrum (Figure S5) analyses, the residue is the unreacted ESO (43.6% of that in feed) or the mixture of unreacted ESO and APBA (33.7% of that in feed), respectively. The GPC results and the obvious increase in torque during the melt-blending process (Figure S1), and the dissolve-precipitation tests, indicate the occurrence of complex reactions in the blend system. The boric acid groups, which are bound to PLA or ESO, readily form boroxine,[20,23] while borate ester can be formed by the reaction between boric acid groups and the hydroxyl groups of PLA or those produced by the opening of the rings in epoxy groups.[22] The possible links by forming boroxine or borate ester in the blend can enhance the interactions between PLA and ESO, which helps to improve the compatibility between them. Moreover, these links allow for the extension of PLA chains to compensate for the decrease in their M_n due to thermal degradation. The resulting enhancement of the interaction between PLA chains may reduce the mobility of the polymer chains, leading to an increase in T_g and a reduction in the crystalline ability of PLA chains. When more APBA (5 phr) is added, the increase of the formed boroxine or borate ester may help to achieve a blend with higher tensile strength. However, the resulting more serious degradation and enhance-

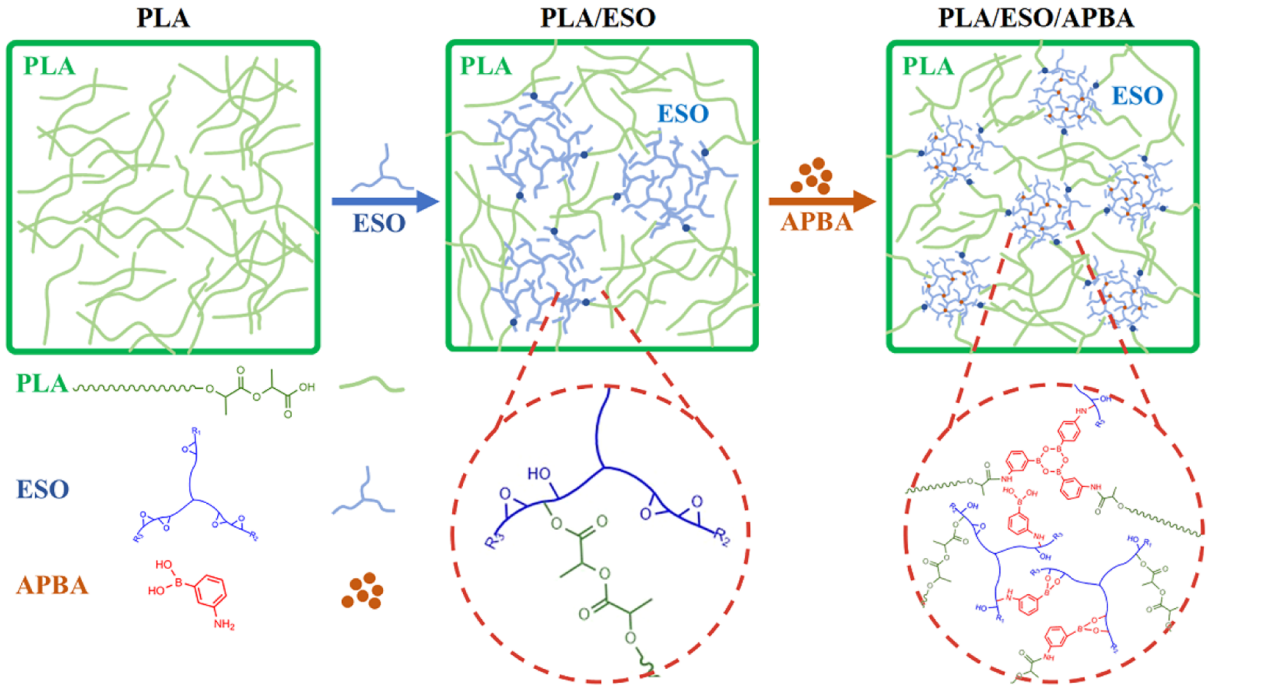

Figure 5. Schematic illustration of the possible reactions between PLA, ESO, and APBA.

https://doi.org/10.1021/acsomega.2c01102
ACS Omega 2022, 7, 17841−17848

ment of the interaction between PLA chains will lead to a significant reduction in elongation at break (Figure S2). Overall, the reaction products of PLA, ESO, and APBA significantly improved the compatibility between PLA and ESO, contributing to a significant enhancement in the mechanical properties of PLA/ESO/APBA blends.

4. CONCLUSIONS

In this study, high-strength, high-ductility PLA-based blends were successfully prepared via the melt-bending of PLA and ESO with APBA. During the blending process, APBA binds with ESO via reaction with the latter's epoxy groups and with PLA chains via aminolysis. Furthermore, in the blends with APBA, the possible borate ester bonds and boroxine structures formed by the boric acid group of APBA may serve as intermolecular links. The reaction products of PLA, ESO, and APBA can significantly improve the compatibility between PLA and ESO, leading to a significant enhancement of the mechanical properties of the blends. With the addition of 3 phr APBA, the yield strength of the PLA/ESO/APBA (90/10/3) blend increases from 56 MPa (without APBA) to 70 MPa. Meanwhile, the elongation at break also reaches 160%, which is far superior to pure PLA (6.5%). Additionally, the links between PLA chains can hinder the movement of PLA chains, leading to a higher T_g and lower crystalline ability of PLA, and a higher blend melt strength compared to PLA/ESO without APBA. These results strongly suggest that, due to their balance between strength and toughness, the PLA/ESO/APBA blends possess great potential toward the manufacture of biomaterials, food packaging, and daily products.

■ ASSOCIATED CONTENT

Supporting Information

The Supporting Information is available free of charge at https://pubs.acs.org/doi/10.1021/acsomega.2c01102.

Change of the torque value in the blend; effect of APBA on the mechanical properties of blends; rheological properties of PLA-based blends; Supporting Information on crystallization properties; and FT-IR and ^{1}H NMR spectra of treated samples (PDF)

■ AUTHOR INFORMATION

Corresponding Author

Jinrong Yao − *State Key Laboratory of Molecular Engineering of Polymers, Department of Macromolecular Science, Laboratory of Advanced Materials, Fudan University, Shanghai 200433, China;* orcid.org/0000-0003-0868-2934; Email: yaoyaojr@fudan.edu.cn

Authors

Jinyu Xie − *State Key Laboratory of Molecular Engineering of Polymers, Department of Macromolecular Science, Laboratory of Advanced Materials, Fudan University, Shanghai 200433, China*

Kai Gu − *State Key Laboratory of Molecular Engineering of Polymers, Department of Macromolecular Science, Laboratory of Advanced Materials, Fudan University, Shanghai 200433, China*

Yan Zhao − *State Key Laboratory of Molecular Engineering of Polymers, Department of Macromolecular Science, Laboratory of Advanced Materials, Fudan University, Shanghai 200433, China*

Xin Chen − *State Key Laboratory of Molecular Engineering of Polymers, Department of Macromolecular Science, Laboratory of Advanced Materials, Fudan University, Shanghai 200433, China;* orcid.org/0000-0001-7706-4166

Zhengzhong Shao − *State Key Laboratory of Molecular Engineering of Polymers, Department of Macromolecular Science, Laboratory of Advanced Materials, Fudan University, Shanghai 200433, China;* orcid.org/0000-0001-5334-4008

Complete contact information is available at: https://pubs.acs.org/10.1021/acsomega.2c01102

Notes

The authors declare no competing financial interest.

■ ACKNOWLEDGMENTS

This work was supported by the National Natural Science Foundation of China (no. 51173028).

■ REFERENCES

(1) Bläsing, M.; Amelung, W. Plastics in soil: Analytical methods and possible sources. *Sci. Total Environ.* **2018**, *612*, 422−435.

(2) Blettler, M. C. M.; Wantzen, K. M. Threats Underestimated in Freshwater Plastic Pollution: Mini-Review. *Water, Air, Soil Pollut.* **2019**, *230*, 174.

(3) Hahladakis, J. N.; Velis, C. A.; Weber, R.; Iacovidou, E.; Purnell, P. An overview of chemical additives present in plastics: Migration, release, fate and environmental impact during their use, disposal and recycling. *J. Hazard. Mater.* **2018**, *344*, 179−199.

(4) Chae, Y.; An, Y.-J. Current research trends on plastic pollution and ecological impacts on the soil ecosystem: A review. *Environ. Pollut.* **2018**, *240*, 387−395.

(5) Zuo, X.; Xue, Y.; Wang, L.; Zhou, Y.; Yin, Y.; Chuang, Y.-C.; Chang, C.-C.; Yin, R.; Rafailovich, M. H.; Guo, Y. Engineering Styrenic Blends with Poly(lactic acid). *Macromolecules* **2019**, *52*, 7547−7556.

(6) Wei, B.; Zhao, Y.; Wei, Y.; Yao, J.; Chen, X.; Shao, Z. Morphology and Properties of a New Biodegradable Material Prepared from Zein and Poly(butylene adipate-terephthalate) by Reactive Blending. *ACS Omega* **2019**, *4*, 5609−5616.

(7) Bian, Y.; Han, C.; Han, L.; Lin, H.; Zhang, H.; Bian, J.; Dong, L. Correction: Toughening mechanism behind intriguing stress−strain curves in tensile tests of highly enhanced compatibilization of biodegradable poly(lactic acid)/poly(3-hydroxybutyrate-co-4-hydroxybutyrate) blends. *RSC Adv.* **2015**, *5*, 34908−34909.

(8) Garlotta, D. A Literature Review of Poly(Lactic Acid). *J. Polym. Environ.* **2001**, *9*, 63−84.

(9) Zhao, J.; Pan, H.; Yang, H.; Bian, J.; Zhang, H.; Gao, G.; Dong, L. Study on miscibility, thermal properties, degradation behaviors, and toughening mechanism of poly(lactic acid)/poly (ethylene-butylacrylate-glycidyl methacrylate) blends. *Int. J. Biol. Macromol.* **2020**, *143*, 443−452.

(10) Kaseem, M. Poly(Lactic Acid) Composites. *Materials* **2019**, *12*, 3586.

(11) Zhao, X.; Hu, H.; Wang, X.; Yu, X.; Zhou, W.; Peng, S. Super tough poly(lactic acid) blends: a comprehensive review. *RSC Adv.* **2020**, *10*, 13316−13368.

(12) Krishnan, S.; Pandey, P.; Mohanty, S.; Nayak, S. K. Toughening of Polylactic Acid: An Overview of Research Progress. *Polym.-Plast. Technol. Eng.* **2016**, *55*, 1623−1652.

(13) Li, D.; Jiang, Y.; Lv, S.; Liu, X.; Gu, J.; Chen, Q.; Zhang, Y. Preparation of plasticized poly (lactic acid) and its influence on the properties of composite materials. *PLoS One* **2018**, *13*, No. e0193520.

(14) Zhao, Y.; Zhao, B.; Wei, B.; Wei, Y.; Yao, J.; Zhang, H.; Chen, X.; Shao, Z. Enhanced compatibility between poly(lactic acid) and poly (butylene adipate-co-terephthalate) by incorporation of N-halamine epoxy precursor. *Int. J. Biol. Macromol.* **2020**, *165*, 460−471.

(15) Nakayama, D.; Wu, F.; Mohanty, A. K.; Hirai, S.; Misra, M. Biodegradable Composites Developed from PBAT/PLA Binary Blends and Silk Powder: Compatibilization and Performance Evaluation. *ACS Omega* **2018**, *3*, 12412−12421.
(16) Mauck, S. C.; Wang, S.; Ding, W.; Rohde, B. J.; Fortune, C. K.; Yang, G.; Ahn, S.-K.; Robertson, M. L. Biorenewable Tough Blends of Polylactide and Acrylated Epoxidized Soybean Oil Compatibilized by a Polylactide Star Polymer. *Macromolecules* **2016**, *49*, 1605−1615.
(17) Bouti, M.; Irinislimane, R.; Belhaneche-Bensemra, N. Properties Investigation of Epoxidized Sunflower Oil as Bioplasticizer for Poly (Lactic Acid). *J. Polym. Environ.* **2022**, *30*, 232−245.
(18) Ali, F.; Chang, Y.-W.; Kang, S. C.; Yoon, J. Y. Thermal, mechanical and rheological properties of poly (lactic acid)/epoxidized soybean oil blends. *Polym. Bull.* **2009**, *62*, 91−98.
(19) Chieng, B.; Ibrahim, N.; Then, Y.; Loo, Y. Epoxidized vegetable oils plasticized poly(lactic acid) biocomposites: mechanical, thermal and morphology properties. *Molecules* **2014**, *19*, 16024−16038.
(20) Yang, Y.; Huang, L.; Wu, R.; Fan, W.; Dai, Q.; He, J.; Bai, C. Assembling of Reprocessable Polybutadiene-Based Vitrimers with High Strength and Shape Memory via Catalyst-Free Imine-Coordinated Boroxine. *ACS Appl. Mater. Interfaces* **2020**, *12*, 33305−33314.
(21) Breuillac, A.; Kassalias, A.; Nicolaÿ, R. Polybutadiene Vitrimers Based on Dioxaborolane Chemistry and Dual Networks with Static and Dynamic Cross-links. *Macromolecules* **2019**, *52*, 7102−7113.
(22) Guo, H.; Yue, L.; Rui, G.; Manas-Zloczower, I. Recycling Poly(ethylene-vinyl acetate) with Improved Properties through Dynamic Cross-Linking. *Macromolecules* **2020**, *53*, 458−464.
(23) Lu, X.; Bao, C.; Xie, P.; Guo, Z.; Sun, J. Solution-Processable and Thermostable Super-Strong Poly(aryl ether ketone) Supramolecular Thermosets Cross-Linked with Dynamic Boroxines. *Adv. Funct. Mater.* **2021**, *31*, 2103061.
(24) Röttger, M.; Domenech, T.; van der Weegen, R.; Breuillac, A.; Nicolaÿ, R.; Leibler, L. High-performance vitrimers from commodity thermoplastics through dioxaborolane metathesis. *Science* **2017**, *356*, 62−65.
(25) Lai, J.-C.; Mei, J.-F.; Jia, X.-Y.; Li, C.-H.; You, X.-Z.; Bao, Z. A Stiff and Healable Polymer Based on Dynamic-Covalent Boroxine Bonds. *Adv. Mater.* **2016**, *28*, 8277−8282.
(26) Pennings, A. J.; Zwijnenburg, A.; Lageveen, R. Longitudinal growth of polymer crystals from solutions subjected to single shear flow. *Kolloid Z. Z. Polym.* **1973**, *251*, 500−501.
(27) Han, Y.; Shi, J.; Mao, L.; Wang, Z.; Zhang, L. Improvement of Compatibility and Mechanical Performances of PLA/PBAT Composites with Epoxidized Soybean Oil as Compatibilizer. *Ind. Eng. Chem. Res.* **2020**, *59*, 21779−21790.
(28) Huang, H.; Chen, L.; Song, G.; Tang, G. An efficient plasticization method for poly(lactic acid) using combination of liquid-state and solid-state plasticizers. *J. Appl. Polym. Sci.* **2018**, *135*, 46669.
(29) Zhang, H.; Zhu, F.; Fu, Q.; Zhang, X.; Zhu, X. Mechanical properties of renewable plasticizer based on ricinoleic acid for PVC. *Polym. Test.* **2019**, *76*, 199−206.
(30) Zhao, T.-H.; Yuan, W.-Q.; Li, Y.-D.; Weng, Y.-X.; Zeng, J.-B. Relating Chemical Structure to Toughness via Morphology Control in Fully Sustainable Sebacic Acid Cured Epoxidized Soybean Oil Toughened Polylactide Blends. *Macromolecules* **2018**, *51*, 2027−2037.
(31) Raghunath, S.; Kumar, S.; Samal, S. K.; Mohanty, S.; Nayak, S. K. PLA/ESO/MWCNT nanocomposite: a study on mechanical, thermal and electroactive shape memory properties. *J. Polym. Res.* **2018**, *25*, 126.
(32) Zhao, Q.; Ding, Y.; Yang, B.; Ning, N.; Fu, Q. Highly efficient toughening effect of ultrafine full-vulcanized powdered rubber on poly(lactic acid)(PLA). *Polym. Test.* **2013**, *32*, 299−305.
(33) Zhang, C.; Huang, Y.; Luo, C.; Jiang, L.; Dan, Y. Enhanced ductility of polylactide materials: Reactive blending with pre-hot sheared natural rubber. *J. Polym. Res.* **2013**, *20*, 1−9.
(34) Sarasua, J.-R.; Prud'homme, R. E.; Wisniewski, M.; Le Borgne, A.; Spassky, N. Crystallization and Melting Behavior of Polylactides. *Macromolecules* **1998**, *31*, 3895−3905.
(35) Yasuniwa, M.; Tsubakihara, S.; Sugimoto, Y.; Nakafuku, C. Thermal analysis of the double-melting behavior of poly(L-lactic acid). *J. Polym. Sci. B Polym. Phys.* **2004**, *42*, 25−32.
(36) Jiang, L.; Wolcott, M. P.; Zhang, J. Study of biodegradable polylactide/poly(butylene adipate-co-terephthalate) blends. *Biomacromolecules* **2006**, *7*, 199−207.
(37) Pan, P.; Inoue, Y. Polymorphism and isomorphism in biodegradable polyesters. *Prog. Polym. Sci.* **2009**, *34*, 605−640.

https://doi.org/10.1021/acsomega.2c01102
ACS Omega 2022, 7, 17841−17848